A Robust Tracking Algorithm Based on Modified Generalized Probability Data Association for Wireless Sensor Network

Long Cheng, Mingkun Xue, Yan Wang, Yong Wang, Yangyang Bi

***Abstract*—Wireless sensor network (WSN) is composed of many micro sensor nodes, and the localization technology is one of the most important applications of WSN technology. At present, many positioning algorithms have high positioning accuracy in line-of-sight (LOS) environment, but poor positioning accuracy in non-line-of-sight (NLOS) environment. In this paper, we propose a modified generalized probability data association algorithm based on arrival of time (TOA). We divided the range measurements into *N* different groups, and each group obtained the corresponding position estimation, model probabilities and covariance matrix of the mobile node through IMM-EKF. We used model probability and hypothesis test to perform NLOS identification for N groups, in which the model probability provided by each group was used for the first NLOS identification, and the innovation and innovation covariance matrix were used for the second NLOS identification in the hypothesis test. Position estimation contaminated by NLOS error is discarded. The correct position estimation is weighted with the corresponding association probability. The simulation and experimental results show that the proposed algorithm can mitigate the influence of NLOS errors and achieve higher localization accuracy when compared with the existing methods.**

***Index Terms*—wireless sensor network; localization; non-line-of-sight; generalized probability data association.**

I. Introduction

Mobile node positioning refers to the use of some method to obtain the coordinate information of the mobile node (MN). The commonly used methods of positioning are mainly divided into two types: ranging and distance-free. The range-based methods mainly include time of arrival (TOA) [1], time difference of arrival (TDOA) [2], received signal strength (RSSI) [3], angle of arrival (AOA) [4], etc. The no-distance methods mainly include a DV-Hop algorithm [5], an APIT algorithm [6], and the like. The signal transmitted directly between the MN and the beacon node (BN), it is called the line-of-sight (LOS) transmission. However, in reality, signals are often not transmitted directly between MN and BNs, but are often blocked by obstacles to reflect or refract, this transmission is called the non-line-of-sight (NLOS) transmission. In the indoor environment, the NLOS situation is particularly serious. Since the transmission distance in the NLOS environment is longer than the propagation distance in the LOS environment, the distance measurement produces a relatively large positive deviation, which is NLOS error. NLOS errors are the main cause of inaccurate positioning.

The Kalman filter (KF) and the improved KF are widely used to solve indoor positioning problems. In [7], the author introduces the GIMM-EKF technique. The Gaussian mixture model (GMM) is used to model the distribution of a set of mixed LOS-NLOS range estimation to obtain the origin state probability. Then, the interaction probability is obtained through the Interacting Multiple Model (IMM) framework. The extended Kalman filter (EKF) is used to filter the position obtained through the interaction probability and distance estimation, and the final result is obtained. In [8], the author proposed the REKF based on robust semi-parametric estimation. The REKF combines regression techniques with EKF to enhance the robustness of EKF in NLOS environments. In [9-11], ranging residuals usually be used to identify NLOS error. In [9], KF and bias KF is performed on the range of the LOS environment and NLOS environment respectively. While a robust extended Kalman filter (REKF) performs a normalized residual test to identify the NLOS measurement in [10]. In [11], based on the linear regression model of the EKF, the BN status is identified and the distance residual is produced at the same time.

Combinational localization algorithm has become a research hotspot for researchers [12-17]. On the purpose of reducing the influence of NLOS, a joint algorithm of genetic algorithm (GA) and iterative least squares (LS) algorithm is proposed in [12]. The GA is used to get a relatively accurate initial value, followed by LS algorithm to get the desired values. In [13], combining received signal strength and time of arrival measurements to mitigate the influence of NLOS biases. In [14], the measured value of the TDOA is first filtered by KF, followed by hyperbolic location algorithm and weighted centroid technique. The Hampel and skipped filters-based weighted least squares (WLS) methods are proposed for situations where the variance for inliers is unknown in LOS/NLOS mixture environments in [15]. In [16], a modified KF algorithm is proposed to reduce the NLOS error, combining least square method (LSM) and particle swarm optimization (PSO), obtaining the location of the target node with higher localization accuracy. In [17], an initial probability estimation is obtained through signal

L. Cheng, M. Xue, Y. Wang and Y. Wang are Department of Computer and Communication Engineering, Northeastern University, Qinhuangdao 066004, Hebei Province, China. (e-mail: chenglong@neuq.edu.cn, mingkunxue61@gmail.com, wangyan_jgxy@neuq.edu.cn, wangyong232513@163.com).

Y. Bi is SANY GROUP CO.,LTD, Changping, 102202, Beijing, China. (biyy@sany.com.cn)

amplitude, followed by an iteratively reweighed least squares regression to classify and reject the NLOS. In [18], by combining the maximum likelihood and the distance distribution with the fingerprint information, combined with the mutual distance and the optimization formula of the fingerprint signal, high-precision indoor positioning can be realized. Eliminating the NLOS transmission situation gradually, then positioning in the LOS propagation environment is introduced in [19], while [20] introducing a transfer function to mitigate the NLOS effect and the propagation channel which contaminated by NLOS can be calibrated back to free space. In [21-23], hierarchical voting is applied to classify and process the NLOS measurements, followed by different process will reduce the influence of NLOS very well. NLOS identification algorithm based on distributed filtering to mitigate NLOS effects is proposed in [24]. In [25], performing a geometric analysis on NLOS and derive a bound that can be used to differentiate NLOS environment. Based on the bound, an identification method is proposed to reduce the influence of NLOS. In [26-29], the authors proposed a WLS estimator, an iterative squared range WLS estimator for mixed LOS/NLOS localization, and a robust LS multilateral technique to mitigate the negative effect of outliers in LOS environments, respectively.

Improve existing positioning algorithms or use novel measurement methods can also achieve better performance. In [30], the author proposes a two-stage closed-form estimator which propose a distance-dependent bias model to derive a range estimation, then followed by trilateration to get the position estimation of the MS. In [31], in order to reduce the NLOS error, the IMM algorithm uses two KFs to smooth range measurements. According to the idea of data fusion, the author proposed an IMM algorithm based on TOA and RSS data fusion to locate the mobile node in [32]. Almost all IMM algorithms need to assume NLOS errors, but in practice, the priori knowledge of the NLOS errors is unknown. The algorithm based on M-estimation and IMM is proposed in [33], which does not require the prior knowledge of the NLOS errors. The MPDA in [34] is a suboptimal filtering algorithm based on Bayesian formula, which can reduce the NLOS error by discarding the position estimation contaminated by NLOS error through NLOS detection. In [35], a position-limited random reasoning algorithm is proposed, which limits the position of nodes to a certain area, so it is helpful for the reasoning algorithm to deal with the important areas of the sample space. In [36], the machine learning method is applied to obtain the measurement under different conditions, and then the deviation between the distance measurement and Euclidean distance is reduced. In [37-38], the Pedestrian Dead Reckoning (PDR) data and the data measured by ultrawide band (UWB) are fused for indoor positioning, and the power consumption of the Inertial Measurement Unit (IMU) is reduced while achieving better positioning accuracy.

In this paper, we propose a robust tracking algorithm based on the modified generalized probabilistic data association (MGPDA) on account of Bayesian estimation criteria. The proposed algorithm has the following advantages:

1) We use the idea similar to Generalized Probability Data Association (GPDA) [39] to test all position estimation, discard those position estimations contaminated by NLOS error, and assign different probabilities to other position estimation. However, different from traditional GPDA, which only uses hypothesis testing for NLOS identification, the MGPDA combines probability detection and hypothesis test for NLOS identification.
2) The MGPDA has the function of double filtering. The MGPDA firstly reduces some NLOS errors by IMM-EKF, and then discards the position estimation contaminated by NLOS errors by NLOS identification, further reduces NLOS errors, so as to realize double filtering.
3) The simulation and experimental results show that the MGPDA proposed can mitigate the influence of NLOS errors when NLOS error obeys different distributions. Without prejudice to the versatility, the proposed localization algorithm in this paper uses TOA measurement, but can be easily extended to other signal features such as TDOA, RSS or AOA.

Both the proposed MGPDA and MPDA are data association algorithms based on Bayesian theory, but there are great differences between them. The MGPDA changes the situation of NLOS identification based on hypothesis test alone, and combines model probability with hypothesis test to improve the correct identification. In the data association, the MPDA defines and divides associated events differently from the MGPDA, and the MPDA does not have the rules that MGPDA algorithm's associated events meet, so they follow different principles when calculating association probability. Since IMM algorithm often does not need NLOS identification when it is used for wireless sensor network localization, so the model probabilities are used to weighted to obtain the final state estimation of mobile node. In fact, according to the value of model probabilities, IMM algorithm can also carry out NLOS identification, so the model probabilities of the IMM can be used for NLOS identification.

The remaining papers are structured as follows. Section II introduces the signal model. The proposed algorithm is explained in Section III, and Section IV illustrates simulation results and experimental results. Conclusions are drawn in Section V.

II. Signal Model

A. Signal model

Assuming that there are M BNs around the MN to track and locate it, we model the state vector of the MN as $\hat{\theta}(k)=\left[x(k)\ y(k)\ \dot{x}(k)\ \dot{y}(k)\right]^T$. $\left(x(k),y(k)\right)$ indicates the two-dimensional position of the MN at time k, $\left(\dot{x}(k),\dot{y}(k)\right)$ indicates the velocity of the MN. The MN moves in two-dimensional coordinates, its motion can be described by the change of the state vector, and the change of the state vector of the MN is modeled as

$$\hat{\theta}(k)=F\hat{\theta}(k-1)+C\varpi(k-1) \tag{1}$$

$$\boldsymbol{F}=\begin{bmatrix}\mathbf{1}&\mathbf{0}&\boldsymbol{\Delta t}&\mathbf{0}\\ \mathbf{0}&\mathbf{1}&\mathbf{0}&\boldsymbol{\Delta t}\\ \mathbf{0}&\mathbf{0}&\mathbf{1}&\mathbf{0}\\ \mathbf{0}&\mathbf{0}&\mathbf{0}&\mathbf{1}\end{bmatrix}\quad \boldsymbol{C}=\begin{bmatrix}\boldsymbol{\Delta t}^2/2&\mathbf{0}\\ \mathbf{0}&\boldsymbol{\Delta t}^2/2\\ \boldsymbol{\Delta t}&\mathbf{0}\\ \mathbf{0}&\boldsymbol{\Delta t}\end{bmatrix}$$

Where Δt is the sampling period. The process noise $\varpi(k)$ is assumed to be the Gaussian white noise with mean zero, covariance matrix $Q(k)$. F is the state transition matrix of the MN. C is the interference noise input matrix. The range measurements between the MN and the M BNs at time k is $D(k)=\left[d_1(k),\ldots,d_M(k)\right]^T$,where $d_m(k)$ is the range measurement obtained by the TOA estimation of the mth BN and the MN multiplied by the speed of light, which is written as

$$\boldsymbol{d_m(k)}=\begin{cases}\boldsymbol{h_m(x(k))+\omega(k)} & \boldsymbol{,if\ \ LOS}\\ \boldsymbol{h_m(x(k))+n_{NLOS}+\omega(k)} & \boldsymbol{,if\ \ NLOS}\end{cases} \quad (2)$$

Where $\omega(k)$ is the Gaussian white noise $N(0,1^2)$,and n_{NLOS} indicates the NLOS error, which could obey different distribution in different kinds of environment. The Euclidean distance between *mth* BN and the MN which is defined as

$$h_m(\hat{\theta}(k))=\sqrt{(x(k)-x_m)^2+(y(k)-y_m)^2}\quad m=1,2,\ldots,M \quad (3)$$

Where (x_m,y_m) represents the two-dimensional coordinates of the *mth* BN, The Euclidean distances between the MN and the M BNs are $h(\hat{\theta}(k))=\left[h_1(k),\ldots,h_M(k)\right]^T$.

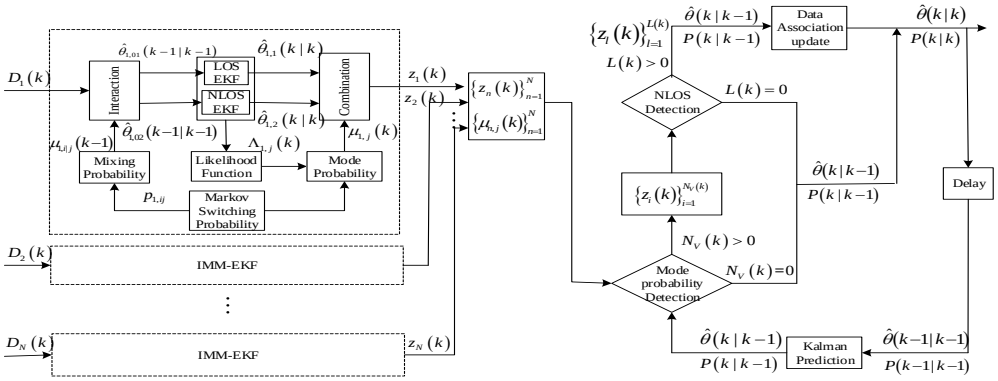

Fig. 1. The flowchart of the MGPDA algorithm.

III. Modified Generalized Probability Data Association

A. The Main Procedures of the Algorithm

The flowchart of the MGPDA algorithm is shown in figure 1. We divide M range measurements into N different groups. Each group obtains a corresponding position estimation $z_n(k)=\left[x_n(k),y_n(k)\right]^T$ and a set of model probabilities $\left[\mu_{n,1}(k),\mu_{n,2}(k)\right]$ which are used for NLOS identification through IMM-EKF. If the BNs in group n and the MN are in LOS environments, the position estimation of group n is of high accuracy. If at least one of the BNs in group n and the MN is in NLOS environment, the position estimation obtained by group n will be interfered by the NLOS factor. Through the IMM-EKF, the MGPDA can mitigate some NLOS errors first. In order to further mitigate the influence of NLOS errors on the position estimation of the MN, we use two methods of model probability and hypothesis test to identify whether $z_n(k)$ is contaminated by NLOS errors. The position estimates contaminated by NLOS errors will be discarded, and the not contaminated by NLOS errors will be regarded as correct position estimates. If the number of correct position estimates is greater than 0, the association probabilities are calculated to update the state estimate, otherwise the predicted state estimate and covariance matrix estimate are taken as the updated state estimates and covariance matrix estimates.

B. Grouping and IMM-EKF estimation

We assume that there are M BNs around the MN to locate it, where M is at least greater than 3. The M BNs are divided into $N=\binom{M}{3}$ different groups, and the position estimation of each group is obtained by IMM-EKF. When using IMM-EKF, the prior probabilities $\mu_{n,j}(k-1)$, the Markov transition probabilities $p_{n,ij}$, prior state $\hat{\theta}_{n,i}(k-1|k-1)$ and covariance matrix $P_{n,i}(k-1|k-1)$ of each group are initialized respectively.

1) *Mixing Probability Calculation* $(i,j=1,2)$

the mixing probabilities of group n is given as

$$\mu_{n,i|j}(k-1|k-1)=(1/\bar{c}_n)\,p_{n,ij}\mu_{n,i}(k-1) \quad (4)$$

$$\bar{c}_n=\sum_i p_{n,ij}\mu_{n,i}(k-1) \quad (5)$$

Where the $\bar{c}_n$ is the normalization factor.

2) *Interacting* $(i,j=1,2)$

The mixing state estimate for group n is modeled as

$$\hat{\theta}_{n,0j}(k-1|k-1)=\sum_i\hat{\theta}_{n,i}(k-1|k-1)\mu_{n,i|j}(k-1|k-1) \quad (6)$$

The mixing covariance matrix for group n is modeled as

$$P_{n,0j}(k-1|k-1)=\sum_i\mu_{n,i|j}(k-1|k-1)\{P_{n,i}(k-1|k-1)+\theta_{n,ij}(k-1|k-1)\cdot\theta_{n,ij}^T(k-1|k-1)\} \quad (7)$$

$$\theta_{n,ij}(k-1|k-1)=\hat{\theta}_{n,i}(k-1|k-1)-\hat{\theta}_{n,0j}(k-1|k-1) \quad (8)$$

3) *Model matched*

The predicted state estimation is defined as

$$\hat{\theta}_{n,j}\left(k\mid k-1\right)=F\hat{\theta}_{n,0j}\left(k-1\mid k-1\right) \tag{9}$$

The predicted covariance matrix estimate is defined as

$$P_{n,j}\left(k\mid k-1\right)=FP_{n,0j}\left(k-1\mid k-1\right)F^{T}+CQ_{n}\left(k\right)C^{T} \tag{10}$$

Where $Q_n(k)$ is process noise covariance matrix. The Jacobian matrix is defined as

$$H_{n,j}\left(k\right)=\frac{\partial h\left(\tilde{\theta}_{n}\left(k\right)\right)}{\partial\tilde{\theta}_{n}\left(k\right)}\Big|_{\hat{\theta}_{n}(k)=\hat{\theta}_{n,j}(k|k-1)} \tag{11}$$

$$v_{n,j}\left(k\right)=D_{n}\left(k\right)-h\left(\hat{\theta}_{n,j}\left(k\mid k-1\right)\right) \tag{12}$$

$$S_{n,j}\left(k\right)=H_{n,j}\left(k\right)P_{n,j}\left(k\mid k-1\right)H_{n,j}^{T}\left(k\right)+R_{n,j}^{*}\left(k\right) \tag{13}$$

Where $v_{n,j}(k)$ is the innovation, $S_{n,j}(k)$ is the innovation covariance matrix. The gain coefficient is given as

$$K_{n,j}\left(k\right)=P_{n,j}\left(k\mid k-1\right)H_{n,j}^{T}\left(k\right)S_{n,j}^{-1}\left(k\right) \tag{14}$$

$$\hat{\theta}_{n,j}\left(k\mid k\right)=\hat{\theta}_{n,j}\left(k\mid k-1\right)+K_{n,j}\left(k\right)v_{n,j}\left(k\right) \tag{15}$$

$$P_{n,j}\left(k\mid k\right)=\left(I_{4}-K_{n,j}\left(k\right)H_{n,j}\right)P_{n,j}\left(k\mid k-1\right) \tag{16}$$

$$\Lambda_{n,j}\left(k\right)=N\left(v_{n,j}\left(k\right);0,S_{n,j}\left(k\right)\right) \tag{17}$$

Where $\hat{\theta}_{n,j}(k\mid k)$ is the updated state estimate, $P_{n,j}(k\mid k)$ is the updated covariance matrix estimate, and $\Lambda_{n,j}(k)$ is the likelihood function.

4) *Model probability update*

The updated model probabilities are modeled as

$$\mu_{n,j}\left(k\right)=\left(1/c_{n}\right)\Lambda_{n,j}\left(k\right)\bar{c}_{n,j} \tag{18}$$

$$c_{n}=\sum_{j}\Lambda_{n,j}\left(k\right)\bar{c}_{n,j} \tag{19}$$

Where c_n is the normalization factor.

5) *Combination*

The updated state estimation of group n is given as

$$\hat{\theta}_{n}\left(k\mid k\right)=\sum_{j}\hat{\theta}_{n,j}\left(k\mid k\right)\mu_{n,j}\left(k\right) \tag{20}$$

The updated covariance matrix of group n is given as

$$P_{n}\left(k\mid k\right)=\sum_{j}\mu_{n,j}\left(k\right)\left\{P_{n,j}\left(k\mid k\right)+\theta_{n,j}\left(k\mid k\right)\cdot\theta_{n,j}^{T}\left(k\mid k\right)\right\} \tag{21}$$

$$\theta_{n,j}=\hat{\theta}_{n,j}\left(k\mid k\right)-\hat{\theta}_{n}\left(k\mid k\right) \tag{22}$$

The position estimation of group n obtained by IMM-EKF is

$$z_{n}\left(k\right)=B\hat{\theta}_{n}\left(k\mid k\right) \tag{23}$$

$$\mathrm{B}=\begin{bmatrix}1&0&0&0\\0&1&0&0\end{bmatrix}$$

Where B is the observation matrix.

C. Algorithm

This section will introduce the MGPDA algorithm as shown in Figure 1 in detail.

1) *Kalman Prediction*

We have assumed that the initial of the state vector and the covariance matrix of the MN are $\hat{\theta}(k-1\mid k-1)$ and $P(k-1\mid k-1)$, the predicted state estimation and covariance matrix estimation are modeled as

$$\hat{\theta}\left(k\mid k-1\right)=F\hat{\theta}\left(k-1\mid k-1\right) \tag{24}$$

$$P\left(k\mid k-1\right)=FP\left(k-1\mid k-1\right)F^{T}+CQC^{T} \tag{25}$$

The predicted position estimation is modeled as

$$z\left(k\mid k-1\right)=B\hat{\theta}\left(k\mid k-1\right) \tag{26}$$

The innovation is defined as

$$v_{n}\left(k\right)=z_{n}\left(k\right)-z\left(k\mid k-1\right)\quad n=1,\ldots,N \tag{27}$$

2) *NLOS Identification*

If all three BNs of group n and the MN are in LOS environments, then

$$v_{n}\left(k\right)\sim N\left(0,S_{n}\left(k\right)\right)\qquad n=1,\ldots,N \tag{28}$$

$$S_{n}\left(k\right)=BP\left(k\mid k-1\right)B^{T}+\sigma_{m}^{2}\left(H_{n}^{T}\left(k\right)H_{n}\left(k\right)\right)^{-1}\ n=1,..,N \tag{29}$$

Where $S_n(k)$ is the innovation covariance matrix. To verify equation (28), we define the following N hypotheses and alternatives,

$$\zeta_{0,n}:v_{n}\left(k\right)\sim N\left(0,S_{n}\left(k\right)\right)\quad n=1,..,N \tag{30}$$

$$\zeta_{1,n}:\text{not }\zeta_{0,n}\quad n=1,\ldots,N \tag{31}$$

We first use the model probabilities obtained by IMM-EKF for NLOS identification. If $\mu_{n,1}(k)$ is not less than $\mu_{n,2}(k)$, $z_n(k)$ is considered a valid position estimate. If $\mu_{n,1}(k)$ is less than $\mu_{n,2}(k)$, $z_n(k)$ will be discarded. We use $N_V(k)$ represent the number of valid position estimates. If $N_V(k)$ is 0, there is no valid position estimation, and hypothesis testing is no longer performed. The algorithm will take the predicted state estimation and covariance matrix estimation as the updated results. If $N_V(k)$ is greater than 0, we use the hypothesis test to perform NLOS identification on all valid position estimates. If the hypothesis $\zeta_{0,i}$ is true, $z_i(k)$ is not contaminated by NLOS errors. If the hypothesis $\zeta_{0,i}$ is rejected, $z_i(k)$ is discarded. In order to determine whether the hypothesis is true, we use adaptive verification gate for NLOS identification. The selection of the threshold γ of the verification area is related to the threshold probability P_G.

$$\int_{0}^{\gamma}f_{\chi^{2}(2)}\left(x\right)dx=P_{G}=1-P_{FA} \tag{32}$$

Where $f_{\chi^2(2)}(\cdot)$ is the chi-square distribution with a degree of freedom of 2, and P_{FA} is the preset false alarm rate. Statistical tests T_i are modeled as

$$T_{i}=v_{i}^{T}\left(k\right)S_{i}^{-1}\left(k\right)v_{i}\left(k\right)\ \ i=1,\ldots,N_{V}\left(k\right) \tag{33}$$

If T_i is not greater than the threshold γ , the hypothesis $\zeta_{0,i}$ is true. We take the position estimate falling into the verification gate as correct position estimate, and record their number as $L(k)$. Otherwise the hypothesis $\zeta_{0,i}$ is rejected. If $L(k)$ is greater than 0, calculate the association probability corresponding to the correct position estimate, and then update the state estimate and the covariance matrix estimate. If $L(k)$ is 0, the predicted state and covariance matrix are used as the updated results.

3) *Data Association*

In order to calculate the association probabilities, we need to define the generalized association events, and the generalized association event needs to satisfy the following rules:

(a) Both the MN and the BNs in subgroup n in the LOS or NLOS environment will obtain the position estimation.

(b) The position estimation from each subgroup comes from the LOS or NLOS environment.

At least one BN in subgroup n and the MN are in the NLOS state, and the position estimation obtained by subgroup n is considered to be from the NLOS environment. Thus, we define the generalized association events as ς_{lt} : { Correct position estimation $z_l(k)$ from the LOS environment }, where $l=1,\ldots,L(k)$, $t=1$. The event ς_{01} denotes that the position estimate $z_l(k)$ from LOS environments was not detected by the verification gate, and the event ς_{l0} indicates that the position estimate was from NLOS environment. The event ς_{00} indicates that there is no position estimate from NLOS environment, which is actually meaningless. The correct position estimate set at time k is defined as $Z(k)=\{z_l(k)\}_{l=1}^{L(k)}$, the correct position estimate set from the initial time to the time k is defined as $Z^k=\{Z(1),Z(2),\ldots,Z(k)\}$.

The probability density function of event ς_{lt} $(l=1,\ldots,L(k),t=1)$ is given as

$$f_{l1}(z_l(k)\mid\varsigma_{l1}(k),L(k),Z^k)=P_G^{-1}N(z_l(k);z(k\mid k-1),S_l(k)) \quad (34)$$

$$=P_G^{-1}\frac{\exp\left\{-\frac{1}{2}v_l^T(k)S_l^{-1}(k)v_l(k)\right\}}{2\pi\left|S_l(k)\right|^{0.5}} \quad (35)$$

The probability density function of event ς_{l0} is given as

$$f_{l0}(z_l(k)\mid\varsigma_{l0}(k),L(k),Z^k)=\frac{L(k)}{V_l(k)}\quad l=1,\ldots,L(k) \quad (36)$$

$$V_l(k)=\pi\gamma\left|S_l(k)\right|^{0.5}\quad l=1,\ldots,L(k) \quad (37)$$

where $V_l(k)$ is the area of the verification region corresponding to the *lth* accepted hypothesis. The probability density function of event ς_{01} is given as

$$f_{01}(z_l(k)\mid\varsigma_{01}(k),L(k),Z^k)=(2V)^{-1}(1-P_dP_G) \quad (38)$$

$$V=\frac{\sum_{l=1}^{L(k)}V_l(k)}{L(k)} \quad (39)$$

Where P_d is the detection probability. The probability density function of the event ς_{00} is

$$f_{00}(z_l(k)\mid\varsigma_{00}(k),L(k),Z^k)=0 \quad (40)$$

The association probabilities are modeled as

$$\beta_{l1}(k)=\frac{1}{c}\left[\xi_{l1}(k)\cdot\prod_{\substack{tr=0\\tr\neq1}}^{1}\sum_{\substack{r=0\\r\neq l}}^{L(k)}\xi_{rtr}(k)+\zeta_{l1}(k)\prod_{\substack{r=0\\r\neq l}}^{L(k)}\sum_{\substack{tr=0\\tr\neq1}}^{1}\zeta_{rtr}(k)\right]$$

$$tr=0,1\ \ r=0,1,\ldots L(k) \quad (41)$$

$$\xi_{lt}(k)=\frac{f_{lt}(z_l(k)\mid\varsigma_{lt}(k),L(k),Z^k)}{\sum_{l=0}^{L(k)}f_{lt}(z_l(k)\mid\varsigma_{lt}(k),L(k),Z^k)} \quad (42)$$

$$\zeta_{lt}(k)=\frac{f_{lt}(z_l(k)\mid\varsigma_{lt}(k),L(k),Z^k)}{\sum_{t=0}^{1}f_{lt}(z_l(k)\mid\varsigma_{lt}(k),L(k),Z^k)} \quad (43)$$

Where c is the normalization factor.

4) *Update*

the innovation covariance matrix $S(k)$ and the Kalman gain $K(k)$ are given as

$$S(k)=BP(k\mid k-1)B^T+\sigma_G^2I_2 \quad (44)$$

$$K(k)=P(k\mid k-1)B^TS^{-1}(k) \quad (45)$$

The updated state $\hat{\theta}(k\mid k)$ and covariance matrix $P(k\mid k)$ are obtained by using the association probabilities.

$$\hat{\theta}(k\mid k)=\hat{\theta}(k\mid k-1)+K(k)\sum_{l=1}^{L(k)}\beta_{l1}(k)v_l(k) \quad (46)$$

$$P(k\mid k)=\beta_{01}(k)P(k\mid k-1)+(1-\beta_{01}(k))P_c(k)+\tilde{P}(k) \quad (47)$$

$$P_c(k)=(I_4-K(k)B)P(k\mid k-1) \quad (48)$$

$$\tilde{P}(k)=K(k)\left[\sum_{l=1}^{L(k)}\beta_{l1}(k)v_l(k)v_l^T(k)-v(k)v^T(k)\right]K^T(k) \quad (49)$$

$$v(k)=\sum_{l=1}^{L(k)}\beta_{l1}(k)v_l(k) \quad (50)$$

IV. Simulation and Experimental Results

This section focuses on the simulation and experiment results. In this paper, six BNs are randomly deployed in the 100 m*100 m area. The MN runs along a fixed trajectory shown in figure 2, and the number of moving steps is 100. the sampling period is $\Delta t=0.5s$, the initial state and covariance matrix of

the MN are set to $\hat{\theta}(0)=\left[1m\ 20m\ 1m/s\ 0.5m/s\right]^T$ and $P(0)=I_4$ .The initial state is set to $\hat{\theta}(0)_{n,j}=\hat{\theta}(0)$, and the initial of covariance matrix is $P(0)_{n,j}=P(0)$ .The initial of Markov transition matrix is $p_{n,ij}=0.5$. The process noise covariance matrix $Q_n(0)=I_2$. The covariance matrix of measurement noise is $R^*(0)_{n.j}=I_3$. The threshold probability is $P_G=0.99$ corresponding to false alarm rate $P_{FA}=0.01$,and the detection probability is set to $P_d=0.95$. In order to simulate NLOS environment, a probability value is generated randomly. Comparing this probability value with the NLOS probability threshold, if the probability is less than the NLOS probability, the MN and the corresponding BNs are considered to be in the NLOS condition. The simulation experiments are carried out under the conditions of NLOS errors obeying Gauss distribution, and exponential distribution respectively. We compare the proposed algorithm with the EKF, REKF, IMM-EKF, RIMM, and MPDA. The simulation results are obtained by 1000 Monte Carlo runs. The root mean square error (RMSE) and the error cumulative distribution function (CDF) of the localization errors are used as the performance for the evaluation algorithm.

$$RMSE=\sqrt{\frac{1}{K}\cdot\frac{1}{MC}\sum_{j=1}^{MC}\sum_{k=1}^{K}\left(\left(\hat{x}_j(k)-x_j(k)\right)^2+\left(\hat{y}_j(k)-y_j(k)\right)^2\right)} \tag{51}$$

Where $\left(\hat{x}_j(k),\hat{y}_j(k)\right)$ is the position estimate obtained during the jth Monte Carlo run and $\left(x_j(k),y_j(k)\right)$ is the real position of the MN at the time of the jth Monte Carlo runtime. $K=100$ is the number of moving steps, $MC=1000$ is the number of Monte Carlo run.

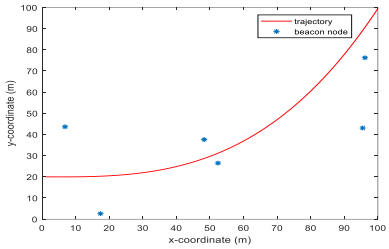

Fig. 2. The trajectory of the mobile node.

A. Gaussian Distribution

It is assumed that the measurement noise obeys the Gaussian distribution $N(0,\sigma_G^2)$ and the NLOS errors obey the Gaussian distribution $N(\mu_{NLOS},\sigma_{NLOS}^2)$. The default parameters of Gaussian distribution are shown in Table I. In the case that the NLOS errors obey the Gaussian distribution, we change one parameter variable each time and keep the other parameters unchanged, so as to explore the influence of the NLOS errors on the positioning accuracy of the algorithms.

TABLE I
GAUSSIAN DISTRIBUTION PARAMETER

Parameter	Symbol	Default Values
the number of beacon nodes	M	6
NLOS error probability	P_{NLOS}	0.5
the measurements noise	$N(0,\sigma_G^2)$	$N(0,1^2)$
the NLOS errors	$N(\mu_{NLOS},\sigma_{NLOS}^2)$	$N(5,6^2)$

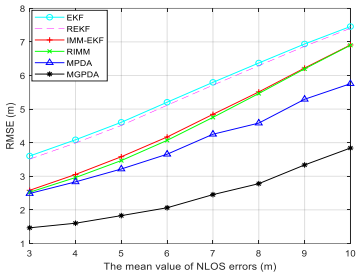

Fig. 3. The RMSE versus the mean value of NLOS errors.

When the mean value of NLOS error varies from 3 to 10, the RMSE of the EKF, REKF, IMM-EKF, RIMM, MPDA, and MGPDA are increasing. The average positioning accuracy of the EKF, REKF, IMM-EKF, RIMM, MPDA and MGPDA are 5.5075m, 5.4250m, 4.6086m, 4.5420m, 4.0092m, and 2.4211m respectively. The average positioning accuracy of MGPDA is about 56.04%, 55.37%, 47.47%, 46.70% and 39.61% higher than that of the EKF, REKF, IMM-EKF, RIMM, and MPDA respectively.

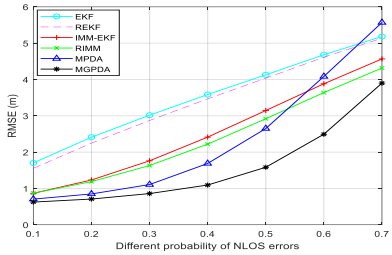

Fig. 4. The RMSE versus different NLOS error probability.

The influence of different NLOS error probabilities on positioning is shown in figure 4. The average positioning accuracy of the EKF, REKF, IMM-EKF, RIMM, MPDA, and MGPDA are 3.5302, 3.4184, 2.5527, 2.3980, 2.3792, and 1.6089, respectively. Compared with the EKF, REKF, IMM-EKF, RIMM, and MPDA, the MGPDA improves the positioning accuracy by 54.42%, 52.93%, 36.97%, 32.91%, and 32.38%, respectively.

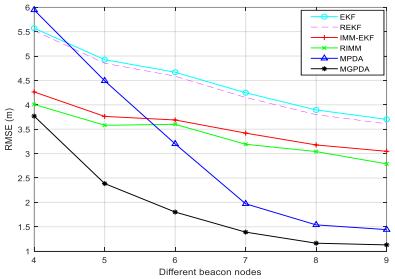

Fig. 5. The RMSE versus the number of beacon nodes.

Figure 5 shows the variation of the RMSE of the EKF, REKF, IMM-EKF, RIMM, MPDA, and MGPDA as the number of beacon nodes increases. The average positioning accuracy of the EKF, REKF, IMM-EKF, RIMM, MPDA, and MGPDA are

4.5011m, 4.4197m, 3.5598m, 3.3683m, 3.0979m, and 1.9396m, respectively. The average positioning accuracy of the MGPDA is 56.91%, 56.11%, 45.51%, 42.42%, and 37.39% higher than that of the EKF, REKF, IMM-EKF, RIMM, and MPDA, respectively.

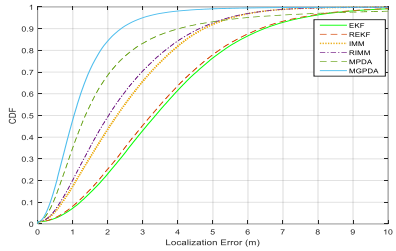

Fig. 6. The CDF of the Localization Error.

From Figure 6, we can see that the 90-percentile localization error of the MGPDA is less than 2.378 m. In comparison, the 90-percentile localization error of the EKF, REKF, IMM-EKF, RIMM, and MPDA is less than 6.460 m, 6.348 m, 4.739 m, 4.611 m, and 4.029 m respectively.

B. Exponential Distribution

It is assumed that the NLOS errors obey exponential distribution $E(\lambda)$. The default parameters of the exponential distribution are shown in the Table II. In the case that the NLOS errors obey the exponential distribution, we change one parameter variable each time and keep the other parameters unchanged, so as to explore the influence of the NLOS errors on the positioning accuracy of the algorithms.

TABLE II
EXPONENTIAL DISTRIBUTION PARAMETER

Parameter	Symbol	Default Values
the number of beacon nodes	M	6
the NLOS error probability	P_{NLOS}	0.5
the measurements noise	$N(0,\sigma_G^2)$	$N(0,1^2)$
the NLOS errors	$E(\lambda)$	$E(8)$

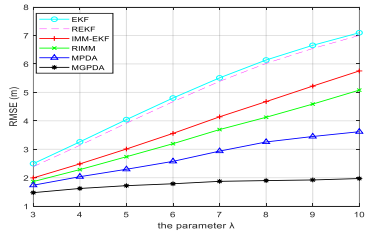

Fig. 7. The RMSE versus the parameter λ.

Through Figure 7, we explore the influence of changing the parameter of the exponential distribution on the RMSE of the EKF, REKF, IMM-EKF, RIMM, MPDA, and MGPDA. The average positioning accuracy of the EKF, REKF, IMM-EKF, RIMM, MPDA, and MGPDA are 4.9993 m, 4.8827 m, 3.8544 m, 3.4458 m, 2.7376 m, and 1.7835 m, respectively. The positioning accuracy of the MGPDA is 64.33%, 63.47%, 53.73%, 48.24%, and 34.85% higher than that of the EKF, REKF, IMM-EKF, RIMM, and MPDA, respectively.

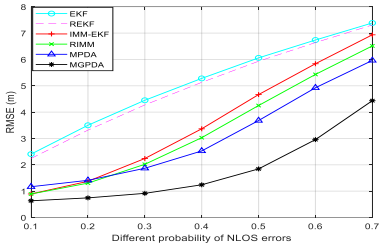

Fig. 8. The RMSE versus different NLOS error probability.

Figure 8 shows the effect of different NLOS errors probabilities on the RMSEs of the EKF, REKF, IMM-EKF, RIMM, MPDA, and MGPDA when the NLOS errors obey exponential distribution. The average positioning accuracy of the EKF, REKF, IMM-EKF, RIMM, MPDA, and MGPDA is 5.1174 m, 5.528 m, 3.6160 m, 3.2058 m, 3.0776 m, and 1.8246m, respectively. Compared with the EKF, REKF, IMM-EKF, RIMM, and MPDA, the MGPDA improves positioning accuracy by approximately 64.35%, 63.53%, 49.54%, 43.08%, and 40.71%, respectively.

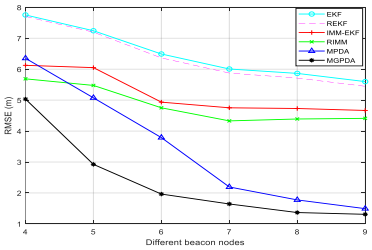

Fig. 9. The RMSE versus the number of beacon nodes.

Figure 9 shows that the RMSEs of EKF, REKF, IMM-EKF, RIMM, MPDA, and MGPDA vary with the number of beacon nodes when the NLOS errors obey the exponential distribution. The average positioning accuracy of the EKF, REKF, IMM-EKF, RIMM, MPDA, and MGPDA are 6.4930 m, 6.3840 m, 5.2100 m, 4.8413 m, 3.4461 m, and 2.3737 m, respectively. The positioning accuracy of MGPDA is 63.44%, 62.82%, 54.44%, 50.97%, and 31.12% higher than that of the EKF, REKF, IMM-EKF, RIMM, and MPDA, respectively.

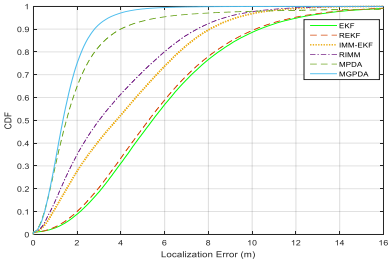

Fig. 10. The CDF of the Localization Error.

From Figure 10, we can see that the 90-percentile of the proposed algorithm is less than 2.792 m. In contrast the 90-percentile of the EKF, REKF, IMM-EKF, RIMM, and MPDA are not more than 10.350 m, 10.150 m, 8.065 m, 7.484 m and 3.988 m, respectively.

C. Experimental results

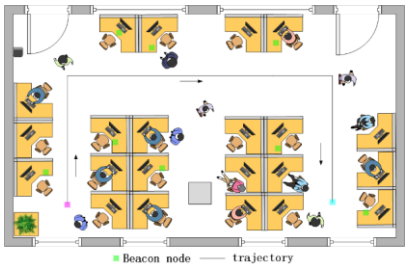

Fig. 11. The deployment of beacon nodes and trajectory of mobile node.

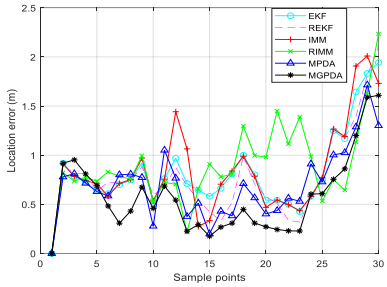

Fig. 12. The localization error of sample points.

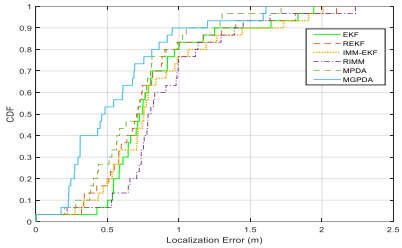

Fig. 13. The CDF of Localization Error.

In order to further verify the positioning accuracy of the proposed algorithm, we carried out experiments in real environment. The Ultra-wideband (UWB) positioning system based on TOA has strong anti-interference ability and high positioning accuracy. The UWB technology is used to transmit signals between BNs and MN to obtain the range measurements. As shown in Figure 11, there are 8 BNs, and the MN moves uniformly along the trajectory. The purple position is the initial position of the MN, the blue position is the end position of the MN, and the green position is the BN position. In order to avoid the reflection of UWB signal from the ground, the MN is moved 1.2m above the ground. The room is 12.6 meters long and 6.6 meters wide. The initial state of MN is set to $\hat{\theta}(0)=\left[1.8m\ \ 6.0m\ \ 0m/s\ \ -0.6m/s\right]^T$. The eight BNs are located at $(x_1=0.5m, y_1=4.1m)$, $(x_2=3.3m, y_2=0.6m)$, $(x_3=3.6m, y_3=3.0m)$, $(x_4=4.2m, y_4=1.2m)$, $(x_5=5.4m, y_5=4.2m)$, $(x_6=9.1m, y_6=1.2m)$, $(x_7=9.6m, y_7=3.6m)$, and $(x_8=11.4m, y_8=5.2m)$ respectively. The MN is sampled by 8 BNs for each 0.6m movement, and the total sampling times are 30. Each BN takes 20 measurements at each sampling point, and the average is taken as the final measurements. Other parameters are the same as the simulation.

The error distribution of each sample point is shown in Figure 12, and the CDF of the localization error is shown in Figure 13. It can be seen from figure 10 that in most cases, the positioning performance of the MGPDA is better than the EKF, REKF, IMM-EKF, RIMM, and MPDA. The 90-percentile of the MGPDA is less than 0.953 m and the CDF tends to one at a localization error of less than 1.609 m. In contrast the 90-percentile of the EKF, REKF, IMM-EKF, RIMM, and MPDA are achieved at 1.249 m, 1.279 m, 1.449 m, 1.387 m and 1.051 m, respectively.

In order to further evaluate the positioning effect of the MGPDA algorithm, we conducted the more experiment in the experimental environment. When the number of BNs is 5, the localization error of sample points is shown in figure 14. Figure 14 shows that the MGPDA algorithm performs better in positioning than other algorithms. When the number of BNs is 6, the localization error of sample points is shown in figure 15, and the average localization error of the EKF, REKF, IMM-EKF, RIMM, MPDA, and MGPDA is 1.311m, 1.351m, 1.310m, 1.303m, 1.257m, and 1.183m, respectively. When the number of BNs is 7, the localization error of sample points is shown in figure 16, and the average positioning accuracy of MGPDA is about 14.23%, 15.62%, 14.45%, 14.88% and 10.64% higher than that of the EKF, REKF, IMM-EKF, RIMM, and MPDA respectively. The more experimental results show that the MGPDA algorithm has good localization performance.

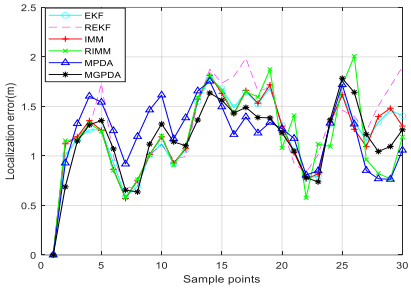

Fig. 14. The localization error of sample points.

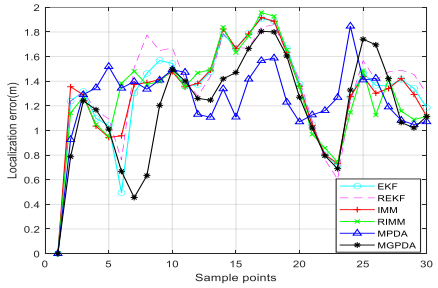

Fig. 15. The localization error of sample points.

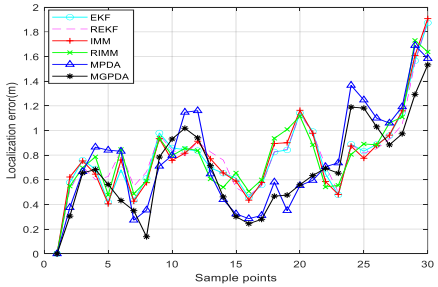

Fig. 16. The localization error of sample points.

V. Conclusion

This paper proposes a modified generalized probabilistic data association algorithm based on TOA measurement for tracking MN in the mixed LOS/NLOS environments. The range measurements are divided into groups, and each group obtains the corresponding position estimation and model probabilities through IMM-EKF. The position estimation is first identified by the model probabilities, and the position estimation contaminated by the NLOS errors is discarded. The retained position estimation is identified by hypothesis test again, and the position estimation with large error is discarded. The correct position estimation is weighted with the association probability to obtain the position estimation of the MN. Simulation results show that the positioning performance of the MGPDA is better than the EKF, REKF, IMM-EKF, RIMM, and MPDA in the mixed LOS / NLOS environments. The MGPDA has high positioning accuracy when the probability of NLOS errors is not large. When the probability of NLOS errors is large, the positioning accuracy of the MGPDA is obviously reduced. Next, we need to further enhance the robustness of the algorithm and improve the positioning accuracy of the MGPDA in the case of large NLOS errors probability.

Acknowledgment

This work was supported by the National Natural Science Foundation of China under Grant No.61803077 and No. 61973069; Natural Science Foundation of Hebei Province under Grant No. F2020501012.

References

[1]. J. Kim, "Non-line-of-sight error mitigating algorithms for transmitter localization based on hybrid TOA/RSSI measurements." *Wireless Networks* (2020) 26:3629–3635.

[2]. B. Yang, Z. Y. Yang, and D. Wang, "A Lagrangian Multiplier Method for TDOA and FDOA Positioning of Multiple Disjoint Sources with Distance an Velocity Correlation Constraints." *Hindawi Mathematical Problems in Engineering* vol 2020.

[3]. P. Thilagavathi, J. M. L. Manickam, "ERTC: an Enhanced RSSI based Tree Climbing mechanism for well-planned path localization in WSN using the virtual force of Mobile Anchor Node." *Journal of Ambient Intelligence and Humanized Computing*, vol 07, Jul, 2020.

[4]. S. Y. Kang, T. Kim and WonZoo Chung, "Hybrid RSS/AOA Localization using Approximated Weighted Least Square in Wireless Sensor Networks." *Sensors* 2020, 20, 1159.

[5]. V. Kanwar, A. Kumar, "DV-Hop localization methods for displaced sensor nodes in wireless sensor network using PSO," *Wireless networks*.

[6]. F. Darakch, G. R. M. Khani, P. Azmi, "CRWSNP: cooperative range-free wireless sensor network positioning algorithm," Wireless Netw (2018) 24:2881-2897.

[7]. W. Cui , B. Li , L. Zhang , and W. Meng, " Robust Mobile Location Estimation in NLOS Environment Using GMM, IMM, and EKF," *IEEE Syst. J.*, vol. 13, no. 3, pp. 3490-3500,Sep. 2019.

[8]. U. Hammes, E. Wolsztynski, and A. M. Zoubir, "Robust tracking and geolocation for wireless networks in NLOS environments," *IEEE J. Sel. Topics Signal Process.*, vol. 3, no. 5, pp. 889–901, Oct. 2009.

[9]. G. L. Zhang, Z. L. Deng, W. Liu, L. G. Li, K. Han, and J. C. Jiao, "An UWB location algorithm for indoor NLOS environment," *IEEE Conf. Ubiquitous Positioning, Indoor Navigation and Location-Based Services (UPINLBS)*, Wuhan, Mar, 2018.

[10]. L. Wang, R. Z. Chen, L. Chen, L. L. Shen, P. Zhang, Y. J. Pan and M. Li, "A Robust Filter for TOA Based Indoor Localization in Mixed LOS/NLOS Environment," *IEEE Conf. Ubiquitous Positioning, Indoor Navigation and Location-Based Services (UPINLBS)*, Wuhan, Mar, 2018.

[11]. Z. Y. Zhang, N. Hu, Y. H. Guo, and X. Yang, "The NLOS Localization Algorithm Based on the Linear Regression Model of Hybrid Filter," The 31th Chinese Control and Decision Conference (2019CCDC), pp. 2242 -2245,2019.

[12]. J. P. Li, L. Zhang, and H. M. Ma, "A New Positioning Method Combining GA and Iterative LS Algorithm in NLOS Environment," *2017 9th IEEE Int Conf. Communication Software and Networks.*, 2017, pp. 403-407.

[13]. J. Kim, " Non-line-of-sight error mitigating algorithm for transmitter localization based on hybrid TOA/RSSI measurements," *Wireless Networks (2020) 26:3629-3635.*

[14]. X. Q. Zhang, and W. Lin, "Hyperbolic-weighted centroid Indoor Location Algorithm based on Kalman Filter," 2018 IEEE 3rd Advanced Information Technology, Electronic and Automation Control Conf (IAEAC 2018)., 2018, pp. 2520-2523.

[15]. C. H. Park, and J. H. Chang, "WLS Localization Using Skipped Filter, Hampel Filter, Bootstrap ping and Gaussian Mixture EM in LOS/NLOS Conditions," *IEEE Access.*, vol.7, pp. 35919-35928,2019.

[16]. Y. Yang, B. K. Li, and B. Ye, "Wireless Sensor Network Localization Based on PSO Algorithm in NLOS Environment," 2016 8th International Conference on Intelligent Human-Machine Systems and Cybernetics., pp. 292-295,2016.

[17]. S. Haigh, J. Kulon, A. Partlow, P. Rogers, and C. Gibson, "A Robust Algorithm for Classification and Rejection of NLOS Signals in Narrowband Ultrasonic Localization Systems," *IEEE Trans. Insterumentation and Measurement*, vol. 68, no. 3, pp. 646-655, Mar, 2019.

[18]. S. N. He, S. H. G. Chan, L. Yu, and N. Liu, "Maxlifd: Joint Maximum Likelihood Localization Fusing Fingerprints and Mutual Distances," *IEEE Trans. Mobile Computing.*, vol. 18, no. 3, pp. 602-617, Mar, 2019.

[19]. L. Cheng, Q. Y. Qi, X. H. Wu, Y. C. Shao, and Y. Wang, "A NLOS Selection based Localization Method for Wireless Sensor Network," *IEEE Int. Conf. Electronics Information and Emergency Commun (ICEIEC)*, Macau, Peoples R CHINA, Jul, 2017.

[20]. M. N. Yang, D. R. Jackson, J. Chen, Z. B. Xiong, and J. T. Williams, "A TDOA Localization Method for Nonline-of-Sight Scenarios," *IEEE Trans.Antennas and Propagation*.,vol.67,no.4,pp.2666-2676,Apr, 2019.

[21]. L. Cheng, J. Q. Hang, Y Wang, and Y. Y. Bi, "A Fuzzy C-Means and Hierarchical Voting Based RSSI Quantify Localization Method for Wireless Sensor Network," *IEEE Access.*, vol.7, pp. 47411-47422,2019.

[22]. L. Cheng, Y. F. Li, Y. Wang, Y. Y. Bi, L. Feng, and M. K. Xue, "A Triple-Filter NLOS Localization Algorithm Based on Fuzzy C-means for Wireless Sensor Networks," *Sensors.*2019,19, 1215.

[23]. Y. Wang, J. Q. Hang, L. Cheng, C. Li, and X. Song, "A Hierarchical Voting Based Mixed Filter Localization Method for Wireless Sensor Network in Mixed LOS/NLOS Environments," *Sensors.* 2018, 18, 2348.

[24]. J. M. Pak, C. K. Ahn, P. Shi, Y. S. Shmaliy, and M. T. Lim, "Distributed Hybrid Particle/FIR Filtering for Mitigating NLOS Effects in TOA-Based Localization Using Wireless Sensor Networks," *IEEE Trans. Industrial Electronics.*, vol. 64, no. 6, pp. 5182-5191, Jun, 2017.

[25]. D. W. Liu, Y. D. Xu, and X. Huang, "Identification of Location Spoofing in Wireless Sensor Networks in Non-Line-of-Sight Conditions," *IEEE Trans Industrial Informatics*., vol. 14, no. 6, pp. 2375-2384, Jun, 2018.

[26]. S. Tiwari, D. Wang, M. Fattouche, and F. Ghannouchi, "A hybrid RSS/TOA method for 3D positioning in an indoor environment," *ISRN Signal Process*., vol. 2012, pp. 1–9, Jan. 2012.

[27]. S. Tomic, M. Beko, M. Tuba, and V. M. F. Correia, "Target localization in NLOS environments using RSS and TOA measurements," *IEEE Wireless Commun. Lett.*, vol.7, no.6, pp.1062-1065, Dec. 2018.

[28]. A. Bahillo, "Hybrid RSS-RTT localization scheme for indoor wireless networks," *EURASIP J. Adv. Signal Process.*,vol.2010, pp.1–12, Mar. 2010.

[29]. H. Chen, G. Wang, and N. Ansari, "Improved Robust TOA-Based Localization via NLOS Balancing Parameter Estimation," *IEEE Trans. Veh. Technol.*, vol. 68, no. 6, pp.6177-6181, Jun. 2019.

[30]. Z. Abu-Shaban, X. Y. Zhou, and T. D. Abhayapala, "A Novel TOA-Based Mobile Localization Technique Under Mixed LOS/NLOS Conditions for Cellular Networks, " *IEEE Trans. Veh Technol.*, vol. 65, no. 11, pp. 8841-8853, 2016.

[31]. P. C. Chen, "A non-line-of-sight error mitigation algorithm in location estimation," in *Proc. IEEE Wireless Communications Networking Conf. (WCNC)*, vol. 1, pp. 316–320, 1999.

[32]. B. S. Chen, C. Y. Yang, F. K. Liao, and J.-F. Liao, "Mobile location estimator in a rough wireless environment using extended Kalman based

IMM and data fusion," *IEEE Trans. Veh. Technol.*, vol. 58, no. 3, pp. 1157–1169, 2009.
[33]. U. Hammes, and A. M. Zoubir, "Robust MT Tracking Based on M-Estimation and Interacting Multiple Model Algorithm," *IEEE Trans. Signal Process.*, vol. 59, no. 7, pp.3398-3409, Jul. 2011.
[34]. U. Hammes and A. M. Zoubir, "Robust mobile terminal tracking in NLOS environments based on data association," *IEEE Trans. Signal Process.*, vol. 51, no. 11, pp. 5872–5882, Nov. 2010.
[35]. R. Mendrzik, and G. Bauch, "Position-Constrained Stochastic Inference for Cooperative Indoor Localization," *IEEE Trans. Signal and Information Processing Networks.*, vol. 5, no. 3, pp.454-468, Sep, 2019.
[36]. V. Barral, C. J. Escudero, J. A. G. Naya, and R. M. Catoira, "NLOS Identification and Mitigation Using Low-Cost UWB Devices", *Sensors.* 2019, 19, 3464.
[37]. M. Pham, D. Yang, and W. H. Sheng, "A Sensor Fusion Approach to Indoor Human Localization Based on Environmental and Wearable Sensors," *IEEE Trans. Automation Science and Engineering.*, vol. 16, no. 1, pp.339-350, Jan, 2019.
[38]. H. C. Wang, X. N. Luo, Y. R. Zhong, and R. S. Lan, "Acoustic Signal Positioning and Calibration with IMU in NLOS Environment," The Eleventh International Conference on Advanced Computational Intelligence, June,2019, Guilin, China.
[39]. Q. Pan, X. N. Ye and H. C. Zhang, "Generalized Probability Data Association Algorithm," *Acta Electronica Sinica*, vol. 33, no. 3, pp. 467-472, 2005.

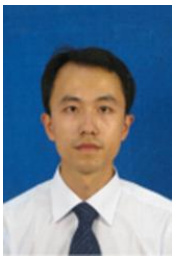

Long Cheng received B.S. degree in automatic control from Qingdao University of Science and Technology, Qingdao, China, in 2008, the M.S. degree in pattern recognition and intelligent system from Northeastern University, Shenyang, China, in 2010. He received Ph.D. degree in pattern recognition and intelligent system from Northeastern University, Shenyang, China, in 2013. Now, he is an associate professor in Northeastern University. His research interests include wireless sensor networks and distributed system.

Mingkun Xue received the B.S degree in communication engineering from Shenyang University of Technology, Shenyang, China in 2018.He is currently persuing M.S degree with Northeastern University, Qinhuangdao, China. His research interest includes research on mobile node location based on wireless sensor network.

Yan Wang was born in Siping, Jilin, China, in 1985. She received B.S. degree in electronic and information engineering from Changchun University of Science and Technology, Changchun, China, in 2007, the M.S. degree in navigation guidance and control from Northeastern University, Shenyang, China, in 2010. She received Ph.D. degree in navigation guidance and control from Northeastern University, Shenyang, China, in 2013. Now, she is an associate professor in Northeastern University. Her research interests include routing and localization algorithm in wireless sensor network.

Yong Wang received B.S. degree in Communication Engineering from AnHui University of Technology, Maanshan, China, in 2019. He is pursing the M.S. degree from Northeastern University, Qinhuangdao, China. His research interests include localization technology in wireless sensor networks.

Yangyang Bi received B.S. degree in Computer Software in 2006 and the M.S. degree in pattern recognition and intelligent system in 2009 from Northeastern University, Shenyang, China. Now, he is the Chief Strategy Officer in SANY GROUP CO.,LTD. He is mainly responsible for the strategic research and strategic management. His research work includes industrial internet of things, wireless sensor network, big data and cloud computing.